A EUROPEAN JOURNAL OF CHEMICAL BIOLOGY

CHEMBIOCHEM

SYNTHETIC BIOLOGY & BIO-NANOTECHNOLOGY

Accepted Article

Title: Bacterial-derived antibody binders as small adapters for DNA-PAINT microscopy

Authors: Thomas Schlichthaerle, Mahipal Ganji, Alexander Auer, Orsolya Kimbu Wade, and Ralf Jungmann

To be cited as: *ChemBioChem* 10.1002/cbic.201800743

Link to VoR: http://dx.doi.org/10.1002/cbic.201800743

A Journal of

ChemPubSoc Europe

WILEY-VCH

www.chembiochem.org

COMMUNICATION WILEY-VCH

Bacterial-derived antibody binders as small adapters for DNA-PAINT microscopy

Thomas Schlichthaerle[a]+, Mahipal Ganji[a]+, Alexander Auer[a], Orsolya Kimbu Wade[a], and Ralf Jungmann*[a]

Abstract: Current optical super-resolution implementations are capable of resolving features spaced just a few nanometers apart. However, translating this spatial resolution to cellular targets is limited by the large size of traditionally employed primary and secondary antibody reagents. Recent advancements in small and efficient protein binders for super-resolution microscopy such as nanobodies or aptamers provide an exciting avenue for the future, however their widespread availability is still limited. To address this issue, we here report the combination of bacterial-derived binders commonly used in antibody purification with DNA-PAINT microscopy. The small size of these protein binders compared to secondary antibodies make them an attractive labeling alternative for emerging super-resolution techniques. We here present a labeling protocol for DNA conjugation of bacterial-derived protein A and G for DNA-PAINT imaging and assay their performance intracellularly by targeting primary antibodies against Tubulin, TOM20, and EGFR and quantify the increase in obtainable resolution.

Super-resolution microscopy is starting to become a standard tool for cell biology research[1]. Several seminal discoveries have been made, which were only feasible by surpassing the classical diffraction limit of light[2]. As recent technical advances in super-resolution are providing sub-5-nm spatial resolution capabilities[3], the size of the labeling probes is becoming increasingly more important.

A popular branch of super-resolution techniques are approaches based on the localization of single molecules[4]. DNA-PAINT is a variation of these single-molecule localization microscopy (SMLM) methods, where the necessary blinking behavior used for downstream super-resolution reconstruction is mediated by the transient hybridization of short dye-labeled oligonucleotides ('imager' strands) which transiently interact with their complementary docking strands on the target of interest[5]. DNA-PAINT possesses several advantages over more traditional SMLM methods such as PALM[6] or STORM[7]. These advantages are mainly based on the fact, that blinking in DNA-PAINT is decoupled from the photophysical properties of dye molecules, thus allowing for the use of bright and photostable dyes rather than ones that efficiently photoswitch. Additionally, the target identity is encoded in the DNA sequence (a programmable probe) similar to a molecular barcode. As the binding interaction between imager and docking strands occurs only transiently, separate imaging rounds can be performed sequentially using different DNA species harboring the same fluorophore, allowing for technically unlimited multiplexing[5b].

However, to apply DNA-PAINT to a question in cell biology, the docking strands need to be "linked" to the target of interest via DNA-conjugated affinity reagents[5b, 8]. The optimal labeling probe should ideally be smaller than the target protein under investigation, allow for quantitative labeling (1:1 stoichiometry), be available for a large variety of targets, and ultimately be cost-effective. A multitude of small binders was recently introduced for super-resolution microscopy. Among them nanobodies[9], aptamer probes[10] or other small protein scaffolds[11]. While these novel binders hold great future promise, antibody-based affinity reagents are – for many applications – still the preferred label for many targets of interest. This is mainly based on the fact that the available probe library vastly exceeds that of any other available binders. However, monoclonal antibodies can be costly and sometimes unavailable in sufficient quantities to perform direct DNA labeling. Immunostaining with secondary antibodies on the other hand adds a large linkage error to the already rather large size of primary antibodies. There is thus a need for small secondary adapter binders.

Previously, nanobodies were reported to bind primary antibodies from mouse and rabbit as host species for super-resolution microscopy[12]. Inspired by this, we here introduce the use of DNA-conjugated bacterial-derived protein A (molecular weight 46 kDa) and G (molecular weight 22 kDa) molecules as small binders for primary antibodies in combination with DNA-PAINT super-resolution microscopy (**Figure 1a, b**). Protein A, derived from *Staphylococcus aureus* has a high affinity to various mammalian IgG molecules (e.g. to IgG1 with ~10 nM) and binds to the Fc-domain, however the binding varies for different species and IgG subclasses [13]. Protein G, derived from *Streptococcus sp.* has a high affinity for various different IgG subclasses from different species and was determined[14] for rat IgG to be ~1 nM. These two proteins are commonly used for antibody purification[15] and were previously applied in immunogold staining for electron microscopy[16] as well asthe attachment of antibodies to DNA nanostructures[17]. Thus, their small size and high affinity makes them an ideal tool for super-resolution microscopy and provides advantages over primary-secondary antibody staining.

Different methods have been introduced to conjugate DNA docking strands to protein-based affinity reagents, where a bifunctional chemical crosslinker was used to react with amino groups or reduced thiols, harboring a reactive moiety which can subsequently react with a modified DNA oligonucleotide[3c, 8, 18]. To produce DNA-modified secondary labeling reagents, protein A from *Staphylococcus aureus* and protein G from *Streptococcus sp.* were conjugated to DNA-PAINT docking strands in a two-step

[a] Thomas Schlichthaerle,+ Dr. Mahipal Ganji,+ Alexander Auer, Orsolya Kimbu Wade, and Prof. Ralf Jungmann
Faculty of Physics and Center for Nanoscience
LMU Munich
Geschwister-Scholl-Platz 1, 80539 Munich and
Max Planck Institute of Biochemistry
Am Klopferspitz 18, 82152 Martinsried
E-mail: jungmann@biochem.mpg.de

[+] These authors contributed equally to this work.

Supporting information for this article is given via a link at the end of the document.

reaction. First, proteins were subjected to react with a TCO-NHS cross-linker and subsequently reacted with commercially available TZ-DNA (see Experimental Section for details). Additionally, protein A and protein G were labeled with NHS-Ester Alexa Fluor™ 647 for diffraction-limited imaging. In order to assess the general feasibility of our labeling approach, we first acquired confocal images of rat anti-alpha-tubulin stained with protein G (labeled with an Alexa647 fluorophore) and rabbit anti-TOM20 protein A conjugates (also labeled with an Alexa647 fluorophore) in A549 cells (**Supplementary Fig. 1**). These immunofluorescence images clearly show specific microtubule and mitochondrial staining, indicating that protein A and protein G can stably and specifically bind to primary rabbit and rat antibodies, respectively. These results made us confident that fluorescently-labeled protein A and protein G could be used as a replacement for secondary antibodies for immunostaining and fluorescence imaging.

We then turned our attention to the DNA-conjugated secondary binders as candidates for DNA-PAINT super-resolution microscopy. As an initial proof-of-concept demonstration for DNA-PAINT imaging with these small bacterial-derived binders, microtubules and TOM20 were chosen for protein G and protein A, respectively. Both targets (**Figure 2**) could be resolved with DNA-PAINT and the resulting images show features well below the diffraction limit (see arrows in **Figure 2b, c**). These datasets are qualitatively similar in performance to typical secondary antibody-based DNA-PAINT data[3c, 5c, 19]. Our first results confirm that protein G and protein A can be used as secondary antibody substitutes. Protein G for rat or rabbit primary antibody targets and protein A for rabbit (**Supplementary Figure 2**). We furthermore assayed binding of protein A and G to primary mouse antibodies and succeeded with specific labeling of EGFR proteins (**Supplementary Fig. 3**). A detailed overview about the possible binding partners of protein A and G that we have assayed in this study can be found in **Supplementary Table 1**. We also checked for potential non-specific binding of protein A and G to cellular targets without primary antibody staining and did not find increased background signals (**Supplementary Fig. 4**).

As we expected to observe a measurable decrease in the observed sizes of targets labeled with these proteins in comparison to primary and secondary antibodies (**Figure 1a**), we next designed experiments to test this hypothesis with DNA-PAINT imaging of EGF surface receptors. The fact that these surface receptors are homogeneously distributed on cell surfaces makes them excellent test candidates for super-resolution imaging. Recently, EGFR was imaged by immunostaining with single-stranded DNA-based aptamers (SOMAmers) with DNA-PAINT super-resolution microscopy to reveal their nanoscale distribution on the cell surface[10a]. To image EGFR using our newly identified small proteins and to compare this with primary and secondary antibody imaging, A549 cells were fixed and immunostained using a monoclonal rabbit antibody against EGFR. As expected, DNA-PAINT super-resolution images of both staining procedures (secondary antibodies and protein A binders) showed homogeneously distributed receptors on the cell surface (**Figure 3a-c** and **h-j**). Two nanoclusters, which were spaced ~80 nm apart could be resolved (**Figure 3d, e**), whereas in comparison to that two nanoclusters for the protein A staining could be visualized which were only 43 nm (**Figure 3k, l**). In order to quantify the size distribution of individual EGFR nanoclusters labeled with secondary antibodies compared to protein A, we aligned thousands of molecules to their center of mass and measured the FWHM of the resulting distributions. The primary-secondary antibody staining approach yielded a considerably larger size distribution (FWHM = 26 nm) compared to the protein A primary antibody approach (FWHM = 13 nm) (**Figure 3f, g, m, n**, see also **Supplementary Fig. 5**). These results demonstrate that the protein A-based labeling is superior to antibody-based labeling in terms of reducing the linkage error in DNA-PAINT imaging.

After the quantification of this reduction of artefacts from labeling probes was achieved with protein A-based labeling, we investigated this achieved reduction in linkage error further in a more challenging 3D imaging application. For this, microtubule structures were chosen, which according to electron microscopy studies[20], have a diameter of ~25 nm. A recent DNA-PAINT study demonstrated that the corona of labeling probes around microtubule filaments can be resolved with super-resolution fluorescence microscopy as a hollow 3D cylinder[21]. Employing this biological system for 3D evaluation of our labeling approach, the potential decrease of the surrounding labeling corona around single microtubule filaments depending on the size of the labeling probe was investigated (**Figure 4**). While both approaches (secondary antibodies and protein G) revealed the expected corona around the microtubules, their diameters were different, as expected. For primary-secondary antibody staining, we obtained a diameter of 57 nm (**Figure 4d, e**), while the protein G-based staining approach resulted in a considerably smaller diameter of 48 nm observed with 3D DNA-PAINT microscopy (**Figure 4i, j**). These results confirmed that using protein G or protein A-based staining as secondary labeling probe yields a smaller linkage error to the true target position in comparison to secondary-antibody staining.

Additionally, we assayed the applicability of using protein A and G in a multiplexed DNA-PAINT imaging experiment. For this, we preincubated DNA-coupled protein A with a primary TOM20 rabbit antibody and DNA-coupled protein G with a primary microtubule rat antibody and removed excess protein A and G binders from the coupled reagents. We then performed simultaneous labeling of TOM20 and microtubules followed by a two-round Exchange-PAINT[5b] experiment using two orthogonal Cy3b imager strands (**Supplementary Fig. 6**) and thus verified that multiplexed imaging is indeed possible.

In conclusion, we extended the use of bacterial-derived binders for immunoglobulins, namely protein A and protein G, as secondary binders for DNA-PAINT microscopy. The key advantage of this approach is that protein A and G are cost-effective, commercially available in much larger quantities compared to secondary antibodies or nanobodies. Additionally, their small size allows for a reduction of the linkage error to the true target position as shown with EGF receptor and microtubule imaging. In the future, these small secondary binders can be evaluated for more species and IgG subclasses, as well as engineered for higher affinity[13b, 22]. In addition, engineering of these proteins to carry unique chemical groups such as cysteines or unnatural amino acids could be employed for quantitative 1:1 labeling of protein to docking strands, which will enable applications in the direction of quantitative imaging such as qPAINT[23].

Experimental Section

Buffer reagents. Buffer C consists of 1xPBS (ThermoFisher Scientific, Cat.No. 20012-019) mixed with 500 mM Sodium Chloride at pH 7.2. *Oxygen Scavenger System – PCD/PCA/Trolox*: 100xPCD (Sigma-Aldrich, Cat. No. P8279-25UN) includes 9.3 mg PCD solved in 13.3 ml of buffer (50% glycerol stock in 50 mM KCL, 1 mM EDTA and 100 mM Tris-HCL at pH 8.0). It is usually stored as 20 µl aliquots at -20 °C; 40×PCA (Sigma-Aldrich, Cat. No. 37580-25G-F) solution includes 154 mg PCA in 10 ml H_2O and is adjusted to pH 9.0 with NaOH. It is stored as 20 µl aliquots at -20 °C; 100×Trolox (Sigma-Aldrich, Cat. No. 238813-1G) solution includes 100 mg Trolox, 430 µl methanol and 345 µl NaOH (1M) in 3.2 ml of H_2O and is aliquoted in 20 µl batches and stored at -20 °C.

Protein A/G labeling via TCO-TZ conjugation. Protein A (Thermo Fisher Scientific, Cat. No. 21181) and protein G (Thermo Fisher Scientific, Cat. No. 21193) were aliquoted at 2.5 mg/ml in 1xPBS and stored at -20 °C. Conjugating single-stranded DNA to protein A or G was performed as described previously for nanobodies[18]. In brief, DNA and proteins were cross-linked using the trans-Cyclooctene (TCO) and methyltetrazin (Tz) coupling reaction. The TZ variant we used was a Tetrazin-PEG5 (Methyltetrazin). The TCO-variant we used was a trans-Cyclooctene-NHS ester ((E)-Cyclooct-4-enyl-2,5-dioxo-1-pyrrolidinyl carbonate). TCO-NHS ester crosslinker (Jena Bioscience, Cat. No. CLK-1016-25) was added at 10x molar excess in 5 µl to the protein and incubated for 2 h at 4 °C on a shaker. Crosslinker aliquots are stored at 10 mg/ml in DMF (Thermo Fisher Scientific, Cat. No. 20673). Subsequently, Zeba Spin Desalting Columns (Thermo Fisher Scientific, Cat. No. 89882) were used to get rid of unreacted crosslinker and TZ-DNA was added at 5x molar excess for 1 h at 20 °C. The final product was buffer exchanged via 10 kDa Amicon Spin Filters (Merck, Cat. No. UFC501096) and used for immunostaining at a concentration of 10 µg/ml.

Protein A/G conjugation with AlexaFluor647 NHS-Ester. Protein A/G were conjugated via AlexaFluor647 NHS-Ester (Thermo Fisher Scientific, Cat. No. A20006) in 10x molar excess for 2 h at 4 °C on a shaker. Conjugated construct was purified from free fluorophore via 10 kDa Amicon Spin Filters (Merck, Cat. No. UFC501096).

Antibody-DNA conjugation. DNA-labeled antibodies were prepared as previously reported[3c]. 300 µl of 1 mg/ml secondary donkey anti-rat antibody (Cat. No. 711-005-152, Jackson ImmunoResearch) were concentrated via 100 kDa Amicon Spin Filters (Cat. No. UFC500396, Merck/EMD Millipore), and volume adjusted to 100 µl in 1xPBS. 10x mole excess over antibody of Maleimide-PEG2-succinimidyl ester crosslinker (Sigma-Aldrich, Cat. No. 746223) in 5 µl DMF was added to the 100 µl of antibody and reacted for 90 min at 4 °C on a shaker in the dark. Afterwards excess crosslinker was removed via zeba desalting spin columns (Cat. No. 89882, Thermo Fisher Scientific). Meanwhile 30 µl of 1 mM Thiol-DNA (solved in H_2O) was added to 70 µl of 250 mM DTT (Cat. No. 20291, Thermo Fisher Scientific) and reduced for 2 h at room temperature on a shaker in the dark. A Nap5 column (Cat. No. 17-0853-02, GE Healthcare) was used to remove DTT from reduced DNA and peak fractions were pooled and concentrated via 3 kDa Amicon Spin Filters (Cat. No. UFC500396, Merck/EMD Millipore). 10x mole excess of DNA was added to the antibody-crosslinker construct and incubated over night at 4 °C on a shaker in the dark. 100 kDa Amicon Spin Filters were used to remove excess DNA and the antibody was adjusted to 100 µl in 1xPBS and stored for further use at 4 °C. Final usage concentration was 10 µg/ml. Secondary anti-rat antibody was conjugated to the P1 Handle. DNA handle and imager sequences can be found in **Supplementary Tables 2** and **3**, respectively.

Cell Culture. A549 cells (ATCC, Cat. No. CRL-1651) or HeLa cells (Leibniz Institute DSMZ: Catalogue of Human and Animal Cell Lines(http://www.dsmz.de), cat. no. ACC-57) were passaged every other day and used between passage number 5 and 20. The cells were maintained in DMEM (ThermoFisher Scientific, Cat. No. 10566016) supplemented with 10 % Fetal Bovine Serum (Thermo Fisher Scientific, Cat. No. 10500-064) and 1 % Penicillin/Streptomycin (Thermo Fisher Scientific, Cat. No. 15140-122). Passaging was performed using 1×PBS and Trypsin-EDTA 0.05 % (Thermo Fisher Scientific, Cat. No. 25300-054). 24 h before immunostaining, cells were seeded on IBIDI 8-well glass coverslips (ibidi, Cat. No. 80827) at 30,000 cells/well. For optimized microtubule imaging, prefixation was performed with prewarmed 0.4% Glutaraldehyde (SERVA, Cat. No. 23115.01) and 0.25% Triton X-100 (Carl Roth, Cat. No. 6683.1) for 90 seconds. Main fixation was performed using 3% glutaraldehyde for 15 min. For imaging of mitochondria, cell surface receptors and microtubule network, 3% paraformaldehyde and 0.1% glutaraldehyde as main fixation without prefixation was performed for 15 min. Afterwards, reduction was done using 1 mg/ml Sodium Borohydride (Carl Roth, Cat. No. 4051.1) in 1×PBS followed by one brief 1xPBS rinse and 3×5 min washing with 1×PBS. Blocking and permeabilization was done for 90 min with sterile filtered 3% (w/v) BSA (Sigma-Aldrich, Cat. No. A4503-10g) and 0.25% (v/v) Triton X-100 in 1×PBS at room temperature. Cells were stained with primary antibodies against tubulin (ThermoFisher Scientific, Cat. No. MA1-80017) or EGFR (Cell Signaling, Cat. No. 4267S or Thermo Fisher Scientific, cat. no. MA5-13319) together with protein A or G overnight on the sample in sterile filtered 3% (w/v) BSA in 1xPBS on a shaker at 4 °C. Cells were washed 3× for 5 min in 1×PBS. For secondary antibody staining, cells were additionally incubated with DNA-labeled anti-rat or anti-rabbit for 1h at room temperature and afterwards washed 3×5 min in 1×PBS. For drift correction purposes, cells were incubated with 1:10 dilution of 90 nm gold particles (cytodiagnostics, Cat. No. G-90-100) in 1×PBS, washed 3×fast and immediately imaged.

Super-resolution microscopy setup. DNA-PAINT was carried out on an inverted Nikon Eclipse Ti microscope (Nikon Instruments) with the Perfect Focus System, applying an objective-type TIRF configuration with an oil-immersion objective (Apo SR TIRF 100×, NA 1.49, Oil). Two lasers were used for excitation: 561 nm (200 mW, Coherent Sapphire) or 488 nm (200 mW, Toptica iBeam smart). The laser beam was passed through a cleanup filter (ZET488/10x or ZET561/10x, Chroma Technology) and coupled into the microscope objective using a beam splitter (ZT488rdc or ZT561rdc, Chroma Technology). Fluorescence light was spectrally filtered with two emission filters (ET525/50m and ET500lp for 488 nm excitation and ET600/50 and ET575lp for 561 nm excitation, Chroma Technology) and imaged on a sCMOS camera (Andor Zyla 4.2) without further magnification, resulting in an effective pixel size of 130 nm after 2×2 binning. Astigmatism for 3D imaging was introduced with the commercial N-STORM Adapter (Nikon Instruments). A second setup was interchangeably used for DNA-PAINT imaging consisting of an inverted Nikon Eclipse Ti 2 microscope (Nikon Instruments) with the Perfect Focus System, applying an objective-type TIRF configuration with an oil-immersion objective (Apo SR TIRF 100×, NA 1.49, Oil). For excitation a 560 nm (2 W, MPB Communication Inc.) was coupled into a single-mode fiber. Using a commercial TIRF Illuminator (Nikon Instruments) the beam was coupled into the microscope body. The laser beam was passed through a cleanup filter (ZET561/10x, Chroma Technology). The beam splitter (ZT561rdc, Chroma Technology) was used. Fluorescence light was spectrally filtered with two emission filters (ET600/50 and ET575lp for 561 nm excitation, Chroma Technology) and imaged on a sCMOS camera (Andor Zyla 4.2) without further magnification, resulting in an effective pixel size of 130 nm after 2×2 binning. Astigmatism for 3D imaging was introduced with the commercial N-STORM Adapter (Nikon Instruments). Imaging parameters can be found in **Supplementary Table 4**.

Confocal Setup. The confocal imaging was performed at the Imaging Facility of Max Planck Institute of Biochemistry, Martinsried, on a ZEISS (Jena, Germany) LSM780 confocal laser scanning microscope equipped with a ZEISS Plan-APO 63x/NA1.46 oil immersion objective.

DNA-PAINT super-resolution microscopy. Cells were imaged using ~3 kW/cm^2 561nm laser excitation. Imager strand concentration varied depending on the measurement from 200 pM – 800 pM Cy3B-P1 and was adjusted to minimize double-binding events. Imaging was performed in 1×PCA (Sigma-Aldrich, Cat. No. 37580-25G-F)/1×PCD (Sigma-Aldrich, Cat. No. P8279-25UN)/1×Trolox (Sigma-Aldrich, Cat. No. 238813-1G) in Buffer C (1×PBS + 500mM NaCl) and imaged for 10.000-50.000 frames at 100-250ms exposure time (see also **Supplementary Table 3**). 3D imaging was performed using an astigmatism lens in the detection path.

Multiplexed imaging with Exchange-PAINT. P5-conjugated protein G was incubated with primary microtubule rat antibody and P1-conjugated protein A was incubated with primary TOM20 rabbit antibody for overnight separately. Unbound protein A and protein G from the coupled reagents was removed by centrifugal filtration using 100 kDa MWCO spin filters (Merck, Cat. No. UFC500396). The coupled reagents were then incubated together with fixed A549 cells for one hour for immunostaining of microtubules and TOM20. The cells were then washed thoroughly with PBS to remove excess protein A/G – antibody reagents and post-fixed using 3% PFA. The cells were imaged using DNA-PAINT super-resolution microscopy in two rounds with a buffer wash in between. In round one, we imaged microtubules using 1.5 nM Cy3B-P5. After washing off free Cy3B-P5, we then introduced 2 nM of Cy3B-P1 to image TOM20.

Image data analysis. Images were reconstructed with the Picasso and SMAP Software Suite. Drift correction was performed with a redundant cross-correlation and/or gold particles as fiducials. Localization precision was determined based on a NeNA analsysis[24].

Acknowledgements

This work was supported by the DFG through the Emmy Noether Program (DFG JU 2957/1-1), the SFB 1032 (Nanoagents for spatiotemporal control of molecular and cellular reactions, Project A11), the ERC through an ERC Starting Grant (MolMap, Grant agreement number 680241), the Max Planck Society, the Max Planck Foundation and the Center for Nanoscience (CeNS) to R.J.. M.G. acknowledges the funding from European Union's Horizon 2020 research and innovation programme under the Marie Skłodowska-Curie grant agreement no 796606.T.S., O.K.W. and A.A. acknowledge support from the DFG through the Graduate School of Quantitative Biosciences Munich (QBM). We thank Sebastian Strauss, Maximilian Strauss, Florian Schueder Alexandra Sophia Eklund and the whole Jungmann lab for fruitful discussion. We also thank Iris Stockmar for initial experiments with the NHS-TCO crosslinking strategy. We also acknowledge the support of the imaging facility at the MPI of Biochemistry.

Keywords: Super-resolution microscopy • Protein binders • DNA Nanotechnology • DNA-PAINT • Single-molecule microscopy

[1] S. J. Sahl, S. W. Hell, S. Jakobs, *Nat Rev Mol Cell Biol* **2017**, *18*, 685-701.

[2] aK. Xu, G. Zhong, X. Zhuang, *Science* **2013**, *339*, 452-456; bJ. Nixon-Abell, C. J. Obara, A. V. Weigel, D. Li, W. R. Legant, C. S. Xu, H. A. Pasolli, K. Harvey, H. F. Hess, E. Betzig, C. Blackstone, J. Lippincott-Schwartz, *Science* **2016**, *354*; cI. Jayasinghe, A. H. Clowsley, R. Lin, T. Lutz, C. Harrison, E. Green, D. Baddeley, L. Di Michele, C. Soeller, *Cell Rep* **2018**, *22*, 557-567.

[3] aM. Dai, R. Jungmann, P. Yin, *Nat Nanotechnol* **2016**, *11*, 798-807; bF. Balzarotti, Y. Eilers, K. C. Gwosch, A. H. Gynna, V. Westphal, F. D. Stefani, J. Elf, S. W. Hell, *Science* **2017**, *355*, 606-612; cJ. Schnitzbauer, M. T. Strauss, T. Schlichthaerle, F. Schueder, R. Jungmann, *Nat Protoc* **2017**, *12*, 1198-1228.

[4] M. Sauer, M. Heilemann, *Chem Rev* **2017**, *117*, 7478-7509.

[5] aR. Jungmann, C. Steinhauer, M. Scheible, A. Kuzyk, P. Tinnefeld, F. C. Simmel, *Nano Lett* **2010**, *10*, 4756-4761; bR. Jungmann, M. S. Avendano, J. B. Woehrstein, M. Dai, W. M. Shih, P. Yin, *Nat Methods* **2014**, *11*, 313-318; cA. Auer, T. Schlichthaerle, J. B. Woehrstein, F. Schueder, M. T. Strauss, H. Grabmayr, R. Jungmann, *Chemphyschem* **2018**, *19*, 3024-3034.

[6] E. Betzig, G. H. Patterson, R. Sougrat, O. W. Lindwasser, S. Olenych, J. S. Bonifacino, M. W. Davidson, J. Lippincott-Schwartz, H. F. Hess, *Science* **2006**, *313*, 1642-1645.

[7] M. J. Rust, M. Bates, X. Zhuang, *Nat Methods* **2006**, *3*, 793-795.

[8] T. Schlichthaerle, A. S. Eklund, F. Schueder, M. T. Strauss, C. Tiede, A. Curd, J. Ries, M. Peckham, D. C. Tomlinson, R. Jungmann, *Angew Chem Int Ed Engl* **2018**, *57*, 11060-11063.

[9] aJ. Ries, C. Kaplan, E. Platonova, H. Eghlidi, H. Ewers, *Nat Methods* **2012**, *9*, 582-584; bM. Mikhaylova, B. M. Cloin, K. Finan, R. van den Berg, J. Teeuw, M. M. Kijanka, M. Sokolowski, E. A. Katrukha, M. Maidorn, F. Opazo, S. Moutel, M. Vantard, F. Perez, P. M. van Bergen en Henegouwen, C. C. Hoogenraad, H. Ewers, L. C. Kapitein, *Nat Commun* **2015**, *6*, 7933.

[10] aS. Strauss, P. C. Nickels, M. T. Strauss, V. Jimenez Sabinina, J. Ellenberg, J. D. Carter, S. Gupta, N. Janjic, R. Jungmann, *Nat Methods* **2018**, *15*, 685-688; bF. Opazo, M. Levy, M. Byrom, C. Schafer, C. Geisler, T. W. Groemer, A. D. Ellington, S. O. Rizzoli, *Nat Methods* **2012**, *9*, 938-939.

[11] C. Tiede, R. Bedford, S. J. Heseltine, G. Smith, I. Wijetunga, R. Ross, D. AlQallaf, A. P. Roberts, A. Balls, A. Curd, R. E. Hughes, H. Martin, S. R. Needham, L. C. Zanetti-Domingues, Y. Sadigh, T. P. Peacock, A. A. Tang, N. Gibson, H. Kyle, G. W. Platt, N. Ingram, T. Taylor, L. P. Coletta, I. Manfield, M. Knowles, S. Bell, F. Esteves, A. Maqbool, R. K. Prasad, M. Drinkhill, R. S. Bon, V. Patel, S. A. Goodchild, M. Martin-Fernandez, R. J. Owens, J. E. Nettleship, M. E. Webb, M. Harrison, J. D. Lippiat, S. Ponnambalam, M. Peckham, A. Smith, P. K. Ferrigno, M. Johnson, M. J. McPherson, D. C. Tomlinson, *Elife* **2017**, *6*.

[12] T. Pleiner, M. Bates, D. Gorlich, *J Cell Biol* **2018**, *217*, 1143-1154.

[13] aT. Moks, L. Abrahmsen, B. Nilsson, U. Hellman, J. Sjoquist, M. Uhlen, *Eur J Biochem* **1986**, *156*, 637-643; bW. Choe, T. A. Durgannavar, S. J. Chung, *Materials (Basel)* **2016**, *9*.

[14] aB. Akerstrom, L. Bjorck, *J Biol Chem* **1986**, *261*, 10240-10247; bU. Sjobring, L. Bjorck, W. Kastern, *J Biol Chem* **1991**, *266*, 399-405.

[15] aP. L. Ey, S. J. Prowse, C. R. Jenkin, *Immunochemistry* **1978**, *15*, 429-436; bS. Hober, K. Nord, M. Linhult, *J Chromatogr B Analyt Technol Biomed Life Sci* **2007**, *848*, 40-47; cE. S. Bergmann-Leitner, R. M. Mease, E. H. Duncan, F. Khan, J. Waitumbi, E. Angov, *Malar J* **2008**, *7*, 129.

[16] F. J. Iborra, A. Pombo, D. A. Jackson, P. R. Cook, *Journal of Cell Science* **1996**, *109*, 1427-1436.

[17] B. J. H. M. Rosier, G. A. O. Cremers, W. Engelen, M. Merkx, L. Brunsveld, T. F. A. de Greef, *Chemical Communications* **2017**, *53*, 7393-7396.

[18] S. S. Agasti, Y. Wang, F. Schueder, A. Sukumar, R. Jungmann, P. Yin, *Chemical Science* **2017**, *8*, 3080-3091.

[19] F. Schueder, J. Lara-Gutierrez, B. J. Beliveau, S. K. Saka, H. M. Sasaki, J. B. Woehrstein, M. T. Strauss, H. Grabmayr, P. Yin, R. Jungmann, *Nat Commun* **2017**, *8*, 2090.

[20] E. Nogales, *Protein Sci* **2015**, *24*, 1912-1919.

[21] Y. Li, M. Mund, P. Hoess, J. Deschamps, U. Matti, B. Nijmeijer, V. J. Sabinina, J. Ellenberg, I. Schoen, J. Ries, *Nat Methods* **2018**, *15*, 367-369.

[22] R. K. Jha, T. Gaiotto, A. R. Bradbury, C. E. Strauss, *Protein Eng Des Sel* **2014**, *27*, 127-134.

[23] R. Jungmann, M. S. Avendaño, M. Dai, J. B. Woehrstein, S. S. Agasti, Z. Feiger, A. Rodal, P. Yin, *Nature Methods* **2016**, *13*, 439.

[24] U. Endesfelder, S. Malkusch, F. Fricke, M. Heilemann, *Histochem Cell Biol* **2014**, *141*, 629-638.

Figures

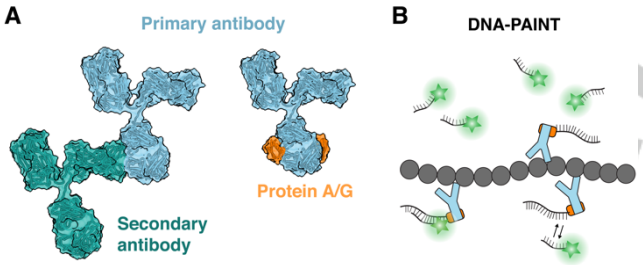

Figure 1 | Small bacterial-derived protein adapters for DNA-PAINT. a) Schematic representation of primary-secondary antibody-based labeling (left) and small bacterial-derived protein adapter labeling (right) highlighting a decrease in overall label size (Modified from pdb IDs: 1fcc & 1igt). b) Schematic representation of the DNA-PAINT concept. Transient hybridization of fluorophore-labeled single-stranded oligonucleotides to their complementary target strands, conjugated to target binders enables programmable super-resolution imaging.

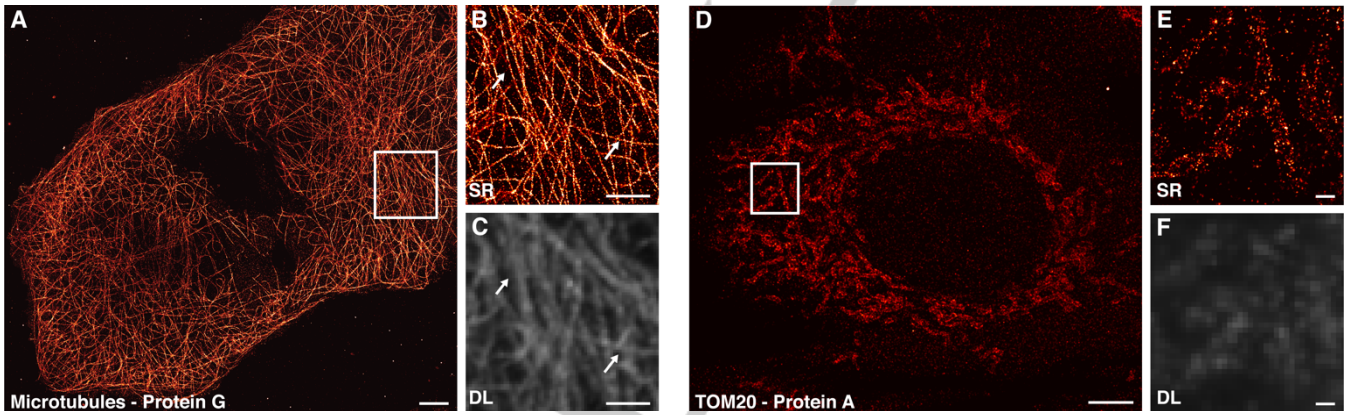

Figure 2 | DNA-PAINT imaging with bacterial-derived protein adapters. a) Microtubule overview super-resolution image in an A549 cell stained with protein G as secondary binder for the rat anti-α-tubulin antibody. b) Zoom in on dense microtubule network, where individual microtubule tracks can be resolved in the DNA-PAINT image but not in the diffraction-limited image c) (white arrows). d) Mitochondria network stained with protein A as secondary binder for rabbit anti-TOM20 antibody. e) Zoom in reveals mitochondrial cavities which could not be observed with diffraction-limited imaging f). Scale bars, 5 µm (a, d), 2 µm (b, c), 500 nm (e, f).

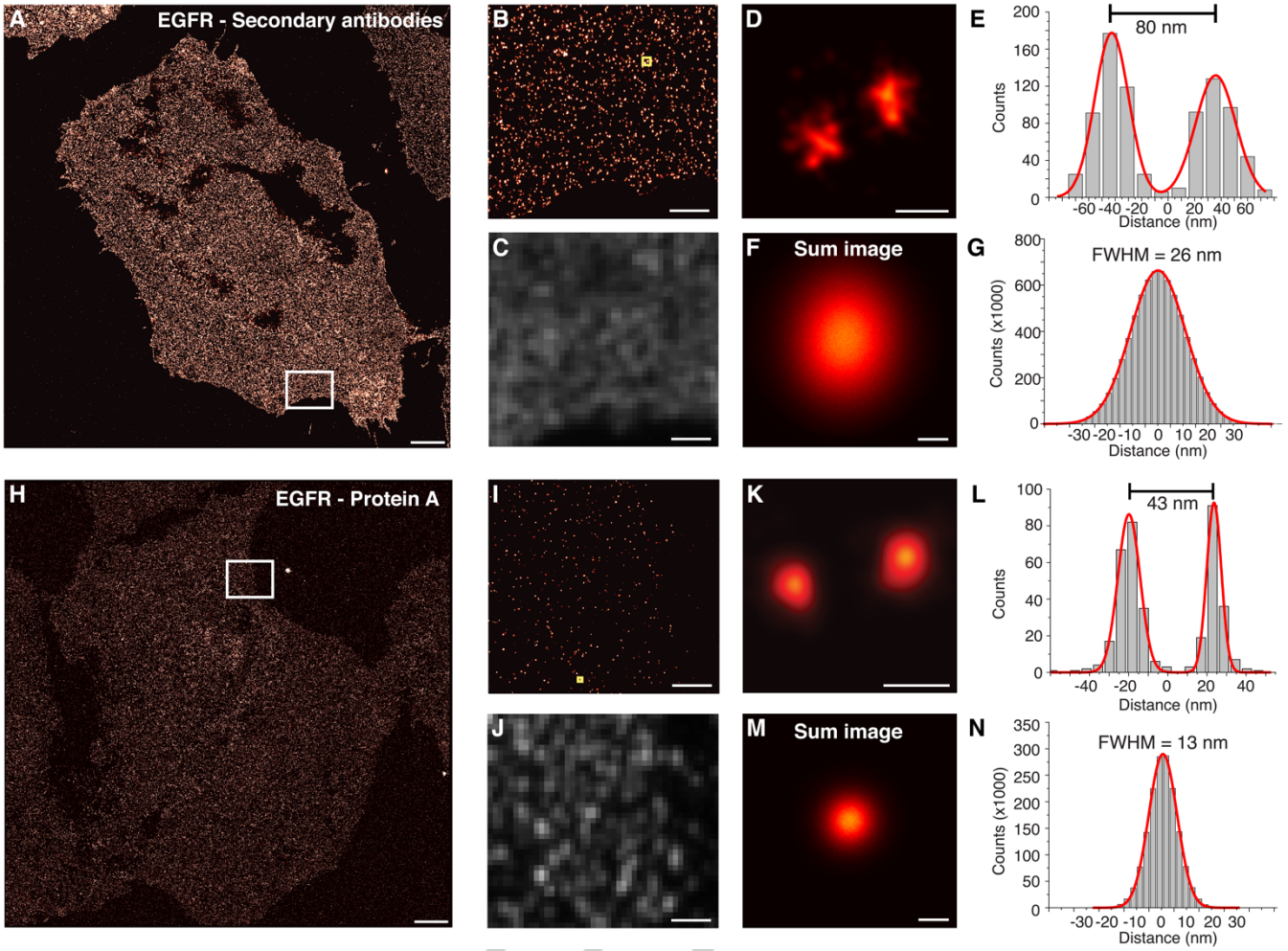

Figure 3 | EGFR nanocluster imaging reveals a decrease in size with small bacterial-derived protein adapters. a) Overview image of EGF receptors in A549 cells labeled with primary-secondary antibodies for DNA-PAINT. b) Zoom in on marked area in a) shows distribution of EGFR nanoclusters, which are not visible in diffraction-limited imaging (c). d, e) Zoom in on two nanoclusters which are ~80 nm apart. Left nanocluster shows a full width half maximum (FWHM) of 30 nm. Right nanocluster a FWHM of 36 nm. f, g) Center-of-mass-aligned nanoclusters stained with primary-secondary antibodies from n=25788 EGFR nanoclusters show a FWHM of 26 nm. h) Overview image of EGF receptors in A549 cells labeled with protein A against the primary rabbit anti-EGF receptor antibody. i) Zoom in on marked area in (h) reveals single spots which are not visible in the diffraction-limited imaging in (j). k, l) Two nanoclusters are 43 nm apart and the left nanocluster reveals a FWHM of 13 nm, the right nanocluster a FWHM of 8.8 nm. m, n) Center-of-mass aligned image of EGF receptor nanoclusters stained with the small bacterial-derived secondary adapter protein A from n=6567 spots show a FWHM of 13 nm. Scale bars, 5 µm (a, h), 1 µm (b, c, I, j), 50 nm (d), 10 nm (f), 25 nm (k), 10 nm (m).

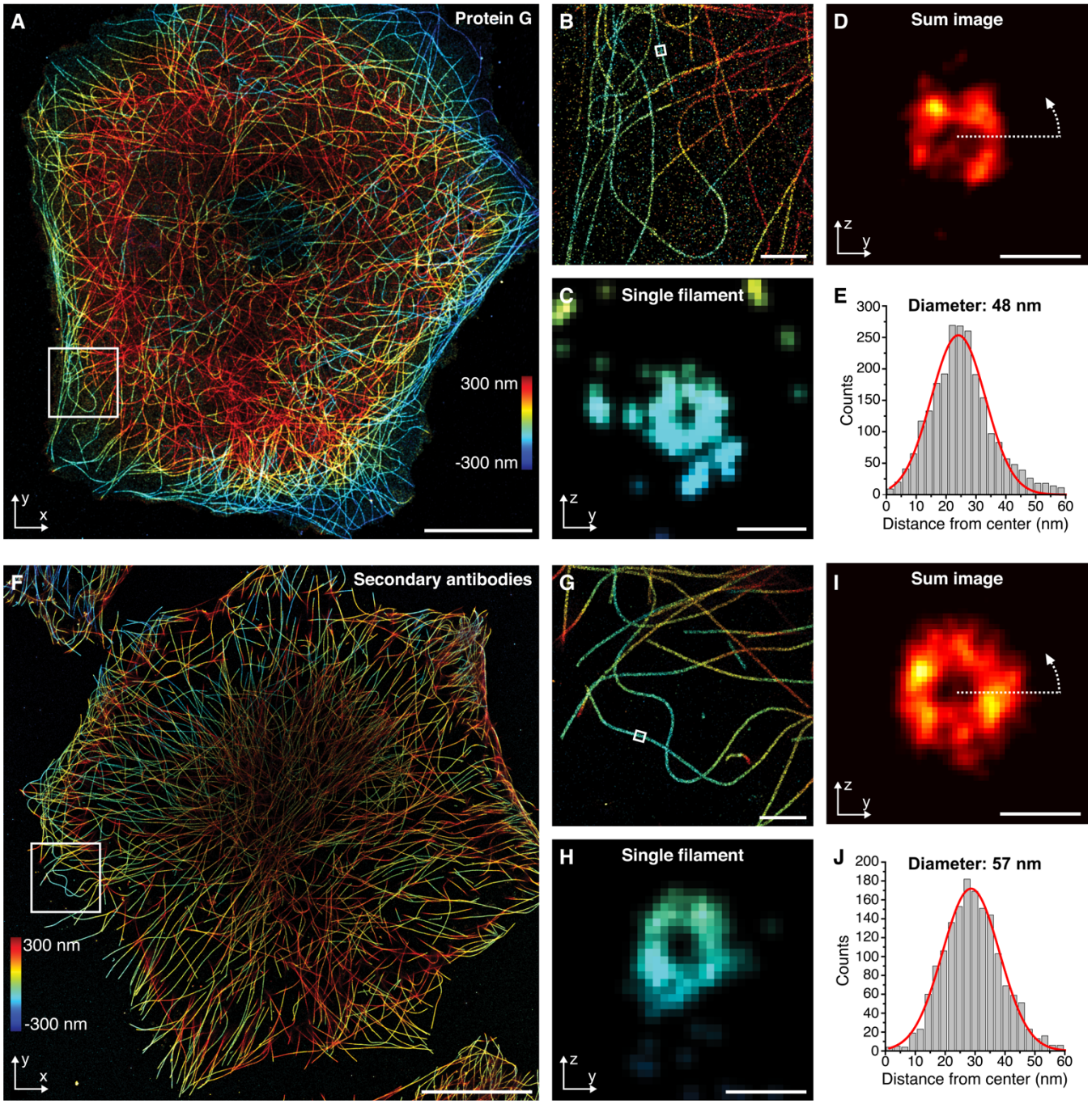

Figure 4 | 3D imaging of microtubules reveals a decrease in diameter with small secondary labeling adapters. a) Overview image of protein G-labeled rat anti-microtubule staining. Color encodes for the Z-height. b) Zoom in on highlighted area in (a) shows a closer view on the microtubule organization. c) Cross-sectional view through a microtubule stretch highlighted in (b). d) Cross-sectional view of average of five microtubules. e) A ring-fit of the average microtubule cylinder shows a diameter of 48 nm (radius 24 nm). f) Overview image of primary-secondary antibody labeled microtubules. g) Zoom in on highlighted area in (h) shows a closer view on the microtubule architecture. i) Microtubule cross-section of highlighted area in (h). j) Cross-sectional view of average of five microtubules. k) An analysis of the diameter of the primary-secondary antibody stained microtubules shows an increased diameter of 57 nm (radius 28.5) in comparison to the small bacterial-derived secondary labeling probe. Scale Bars: 10 µm (a, f), 1 µm (b, g), 50 nm (c, d, h, i).

Entry for the Table of Contents

COMMUNICATION

Bacterial-derived small secondary antibody binders protein A and G are employed to reduce linkage errors in super-resolution microscopy with DNA-PAINT

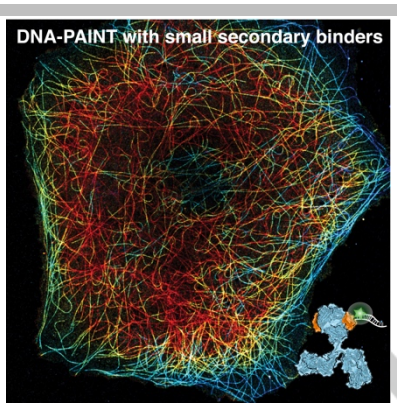

*Thomas Schlichthaerle, Mahipal Ganji, Alexander Auer, Orsolya Kimbu Wade, Ralf Jungmann**

Page No. – Page No.

Bacterial-derived antibody binders as small adapters for DNA-PAINT microscopy